Spin transport in $CH_3NH_3PbI_3$

2014 J. Phys. D: Appl. Phys. 47 405002

(http://iopscience.iop.org/0022-3727/47/40/405002)

IOP Publishing Journal of Physics D: Applied Physics

J. Phys. D: Appl. Phys. **47** (2014) 405002 (5pp) doi:10.1088/0022-3727/47/40/405002

Spin transport in $CH_3NH_3PbI_3$

Qingyu Xu[1,2,4], Er Liu[1], Sai Qin[1], Shan Shi[3], Kai Shen[3], Mingxiang Xu[1], Ya Zhai[1] and Shuai Dong[1,4]

[1] Department of Physics, Southeast University, Nanjing 211189, and Key Laboratory of MEMS of the Ministry of Education, Southeast University, Nanjing 210096, and Collaborative Innovation Center of Suzhou Nano Science and Technology, Soochow University, Suzhou 215123, People's Republic of China
[2] National Laboratory of Solid State Microstructures, Nanjing University, Nanjing 210093, People's Republic of China
[3] School of Materials Science and Technology, Nanjing University of Aeronautics and Astronautics, Nanjing 210016, People's Republic of China

E-mail: xuqingyu@seu.edu.cn and sdong@seu.edu.cn

Received 10 June 2014, revised 19 July 2014
Accepted for publication 29 July 2014
Published 4 September 2014

Abstract

Organometal trihalide perovskites with the general formula $(CH_3NH_3)PbX_3$ (X is Cl, I and/or Br) have a composition dependent tunable band gap and long electron–hole diffusion length, which is not only being hotly studied for usage in hybrid solar cells, but also has potential application in organic spintronics. In this work, we prepared $CH_3NH_3PbI_3$-coated Fe_3O_4 granular films. $CH_3NH_3PbI_3$ behaves effectively as a spacer to decouple the Fe_3O_4 particles and spin-preserved transporting matrix. The magnetoresistance of Fe_3O_4 particles has been significantly enhanced after $CH_3NH_3PbI_3$ coating, which is about -6% at 300 K and -10.8% at 150 K under a magnetic field of 10 kOe, about 3 times larger than the values of pure Fe_3O_4 (-1.9% at 300 K and -3.4% at 150 K).

Keywords: spintronics, organometal trihalide perovskites, magnetoresistance

(Some figures may appear in colour only in the online journal)

Electrons possess two degrees of freedom: charge and spin. In contrast to the electrical control of charge in conventional semiconductor microelectronics, spintronics allows the simultaneous control of both charge and spin. After the observation of giant magnetoresistance in metallic multilayers [1], the fast development of spintronics has also been extended to organic materials, so-called organic spintronics. Spintronics generally has three main components: the generalization, transport and detection of spin polarization [2]. In organic spintronics, inorganic materials with high spin polarization (P), such as Fe_3O_4 [3], $La_{0.67}Sr_{0.33}MnO_3$ [4], etc., have always been used for the generalization of spin polarization, due to the lacking of ferromagnetic (FM) organic materials, especially at room temperature. The organic molecules have long spin relaxation times and coherent length due to weak spin–orbit coupling and hyperfine interaction [5], and have been always used as spacers to decouple the FM electrodes, while allowing the spin transport from one contact to the other [6].

[4] Authors to whom any correspondence should be addressed.

Conventional organic materials, such as oleic acid [3], tetraphenyl porphyrin (TPP) and aluminum tris(8-hyroxyquinoline) (Alq3) [4, 5], etc., have been used in organic spintronics. However, the deposition of the FM layer on an organic spacer has a shortcoming that FM atoms have high kinetic energy and are easy to penetrate into the organic layer to form the ill-defined layer [5]. Recently, organometal trihalide perovskites with the general formula $(CH_3NH_3)PbX_3$ (X is I, Br andor Cl) have attracted intensive research interests due to their successful application in hybrid solar cells with high power conversion efficiency [7, 8]. The long electron–hole diffusion length ($\sim$100 nm) suggests the possible long spin coherence length [9]. The perovskite structure taking the form of ABX_3 ($A = CH_3NH_3^+$; $B = Pb^{2+}$; and $X = Cl^-$, I^- and/or Br^-), which is a common framework in inorganic materials, is expected to have better compatibility with inorganic FM contacts and more resistance on the penetration of FM atoms during the deposition. Until now the report on the spintronics application of organometal trihalide perovskites is still lacking. In this paper, we prepared the $CH_3NH_3PbI_3$-coated Fe_3O_4 granular films, and observed strongly enhanced

magnetoresistance (MR) compared with that of pure Fe_3O_4, which demonstrates the promising application of $CH_3NH_3PbI_3$ in spintronics.

The Fe_3O_4 particles were prepared by the solvothermal reduction method [10]. The $CH_3NH_3PbI_3$ precursor solution was prepared, following the reported procedure [9]. Several drops of $CH_3NH_3PbI_3$ precursor solution were added to the Fe_3O_4 powders. After ultrasonication the mixture was moved to a cleaned glass substrate, and spread out to make a uniform film. Finally the sample was kept in a drying oven at 90 °C for about 15 min The structure was characterized by x-ray diffraction (XRD, Rigaku SmartLab3). The morphology was observed by scanning electron microscopy (SEM, FEI Inspect F50), and the compositions were determined by energy dispersive x-ray spectroscopy (EDS) attached to SEM. The magnetization was measured by a vibrating sample magnetometer integrated into a physical property measurement system (PPMS-9, Quantum Design). The field and temperature dependent resistance were measured using the four-terminal method by a home-made measuring system with a temperature down to 5 K and a field up to 10 kOe.

Figure 1 shows the XRD patterns of Fe_3O_4 particles before and after the $CH_3NH_3PbI_3$ coating. As can be clearly seen, Fe_3O_4 particles have the single phase of spinel structure with the lattice constant of 8.363 Å, close to the bulk value (PDF#65–3107). It should be noted that impurity phase of PbI_2 might sometimes be observed in the $CH_3NH_3PbI_3$ film [11]. Except for the observed peaks corresponding to the Fe_3O_4 phase in $CH_3NH_3PbI_3$-coated Fe_3O_4, the rest peaks can all be indexed to $CH_3NH_3PbI_3$ without any impurity phase, suggesting the high quality of our samples [8]. The calculated crystal size of Fe_3O_4 from the XRD pattern is about 25 nm.

The morphology of samples was studied by SEM, as shown in figure 2. Fe_3O_4 particles clearly show a spherical shape, similar to the previous report [10]. However, by carefully inspecting Fe_3O_4 particles with larger magnification, the surface is not smooth and has many holes. The Fe_3O_4 particles are the aggregation of many small crystals, indicating the polycrystalline nature. After the $CH_3NH_3PbI_3$ coating, there is no significant morphology change (figure 2(*b*)). The capping layer of $CH_3NH_3PbI_3$ cannot be clearly resolved in the SEM image. The cross-sectional image (figure 2(*c*)) shows that the film is rather uniform with a thickness of about 6 μm. The inset shows the enlarged view, confirming the close packing of coated Fe_3O_4 particles without significant aggregation of $CH_3NH_3PbI_3$. The chemical compositions have been studied by EDS. Besides the Fe and O from Fe_3O_4 particles, I and Pb can also be clearly resolved, confirming the coating of $CH_3NH_3PbI_3$ on Fe_3O_4 particles. The averaged weight and atomic ratio of each element is listed in the inset of figure 2(*d*). The weight ratio between Fe_3O_4 and $CH_3NH_3PbI_3$ is about 1:0.09. The density of $CH_3NH_3PbI_3$ is calculated to be 1.03 g cm^{-3} [8]. Considering the density of Fe_3O_4 (5.2 g cm^{-3}), the particle size will increase from 450 nm in diameter to 510 nm after the $CH_3NH_3PbI_3$ coating. Thus, the thickness of the $CH_3NH_3PbI_3$ shell is estimated to be about 30 nm in average, although the value may vary a little from particle to particle.

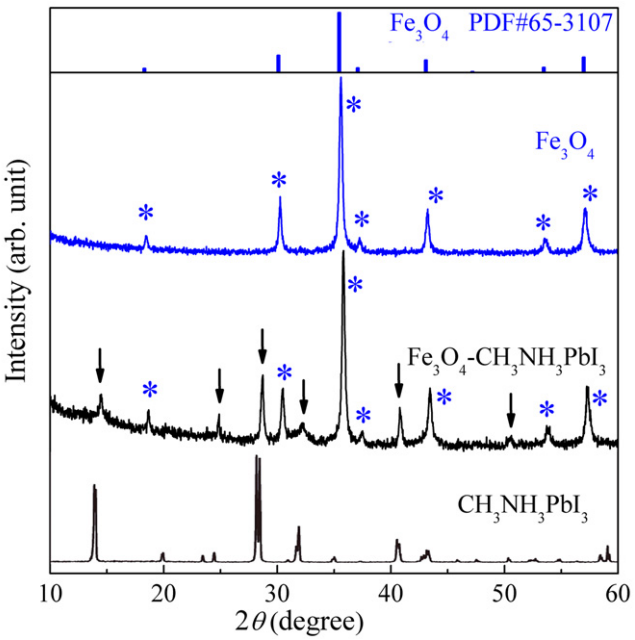

Figure 1. The XRD patterns of Fe_3O_4 particles with and without $CH_3NH_3PbI_3$ coating. The '*' and arrows mark the diffraction peaks from Fe_3O_4 and $CH_3NH_3PbI_3$, respectively. The XRD pattern of Fe_3O_4 (PDF#65–3107) and $CH_3NH_3PbI_3$ (from [8] are also shown).

Figure 3 shows the field dependent magnetization (M–H) curves of Fe_3O_4 particles with and without the $CH_3NH_3PbI_3$ coating. Fe_3O_4 is a well known ferrimagnetic material with a cubic inverse spinel structure and a net magnetic moment of 4 μ_B/f.u. [12]. The well saturated M–H curve with a small coercivity of about 40 Oe is observed for Fe_3O_4 particles. The saturated magnetization (M_s) (84 emu g^{-1}) is consistent with the previous reported value on Fe_3O_4 particles prepared by the same method [10]. After the $CH_3NH_3PbI_3$ coating, a similar M–H curve can be observed with a smaller M_s (65 emu g^{-1}), which is due to the addition of nonmagnetic $CH_3NH_3PbI_3$. However, the M_s is smaller than the expected value (77 emu g^{-1}) by taking into account the weight ratio determined by EDS (the mass ratio between Fe_3O_4 and $CH_3NH_3PbI_3$ determined by M_s is 1 : 0.3). One possible reason for this discrepancy might be that the $CH_3NH_3PbI_3$ solution tended to accumulate at the bottom of the film due to the influence of gravity, leading to the higher concentration of $CH_3NH_3PbI_3$ close to the substrate surface, while EDS can only detect the chemical composition at the top region of the film due to the penetration length limit of electrons in SEM. To confirm this assumption, we dissolved the coating $CH_3NH_3PbI_3$ in anhydrous N,N-Dimethylformamide (DMF). The mass ratio of Fe_3O_4 and $CH_3NH_3PbI_3$ was determined to be 1:0.25, which is quite close to the value determined by M_s. The slight difference might be due to the uncompleted removal of the coated $CH_3NH_3PbI_3$. However, the possible modification of M_s by organic coating cannot be excluded, which needs further studies [13, 14].

The temperature dependent resistance (R–T) for Fe_3O_4 particles with and without $CH_3NH_3PbI_3$ coating was measured by applying a constant current, shown in figure 4. Due to the too high resistance of $CH_3NH_3PbI_3$-coated Fe_3O_4

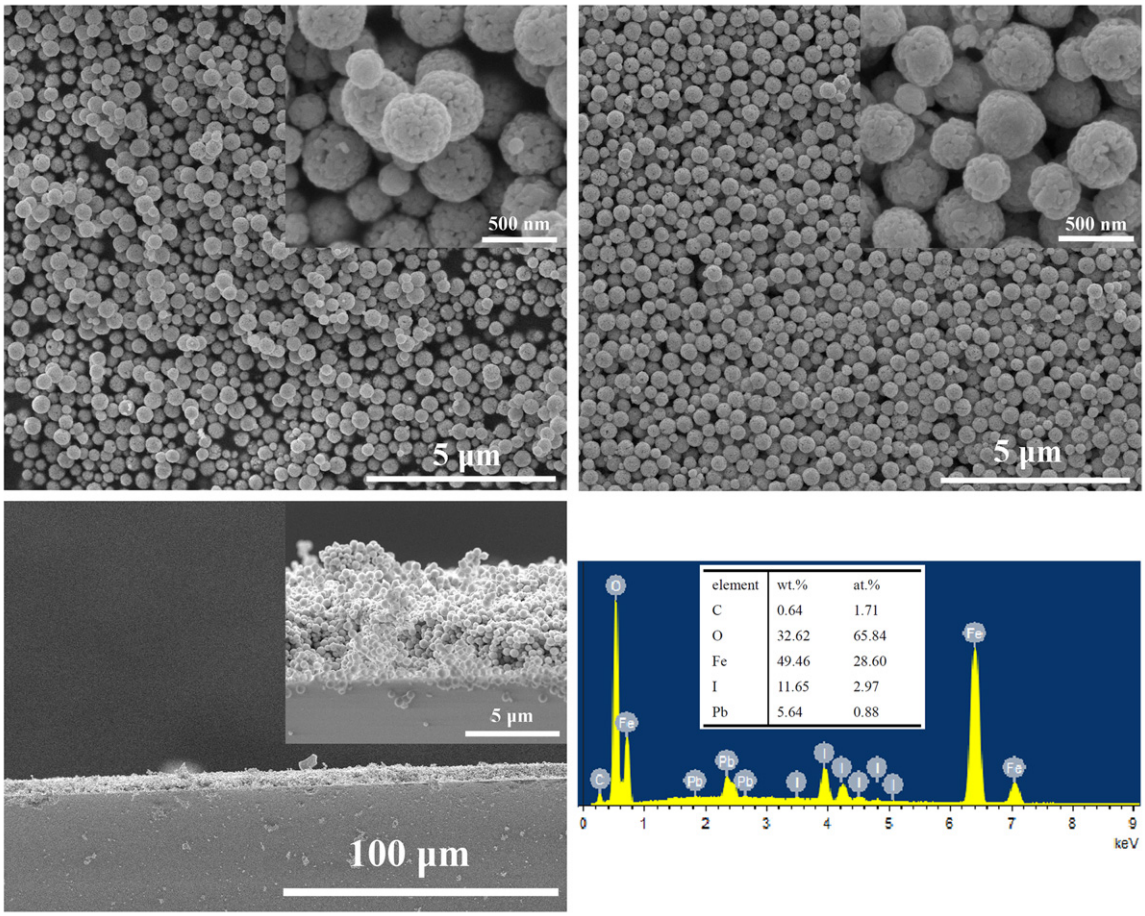

Figure 2. The SEM images for (*a*) pure Fe_3O_4 particles, (*b*) plane view and (*c*) cross-section view for $CH_3NH_3PbI_3$-coated Fe_3O_4 particles. The insets are the magnified images. (*d*) EDS spectrum for $CH_3NH_3PbI_3$-coated Fe_3O_4 particles, the inset shows the weight and atomic concentrations.

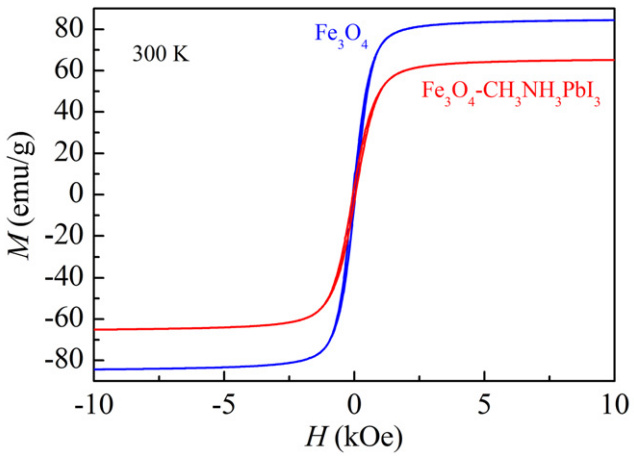

Figure 3. The M–H curves for Fe_3O_4 particles with and without $CH_3NH_3PbI_3$ coating at 300 K.

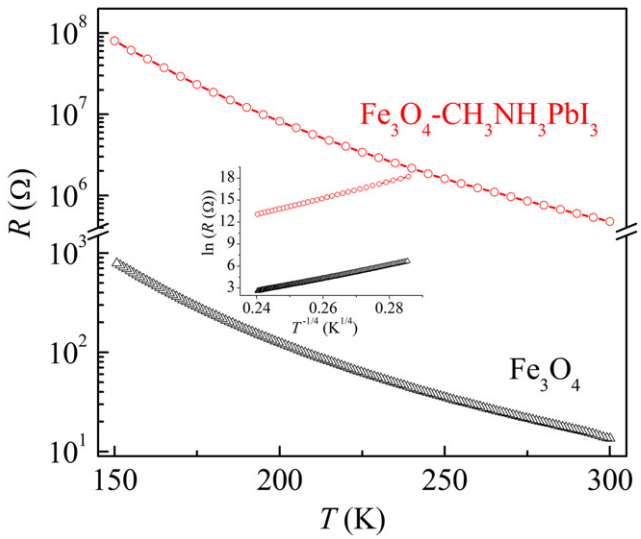

Figure 4. The temperature dependent resistance for Fe_3O_4 particles with and without $CH_3NH_3PbI_3$ coating. The inset shows the dependence of $\ln(R)$ on $T^{-1/4}$.

particles at low temperatures which increases drastically with decreasing temperature, we only measured the resistance down to 150 K. The resistance of $CH_3NH_3PbI_3$-coated Fe_3O_4 is about five orders of magnitude higher than that of pure Fe_3O_4, indicating that the resistance mainly arises from $CH_3NH_3PbI_3$. The resistance of both samples closely follows the $\ln R \sim T^{-1/4}$ relation (shown in the inset), suggesting the variable range hopping among localized states of molecules or grain boundaries [3]. Compared with the pure Fe_3O_4 particles, the well decoupling between the particles indicates that the improvement of MR in $CH_3NH_3PbI_3$-coated Fe_3O_4 particles can be expected.

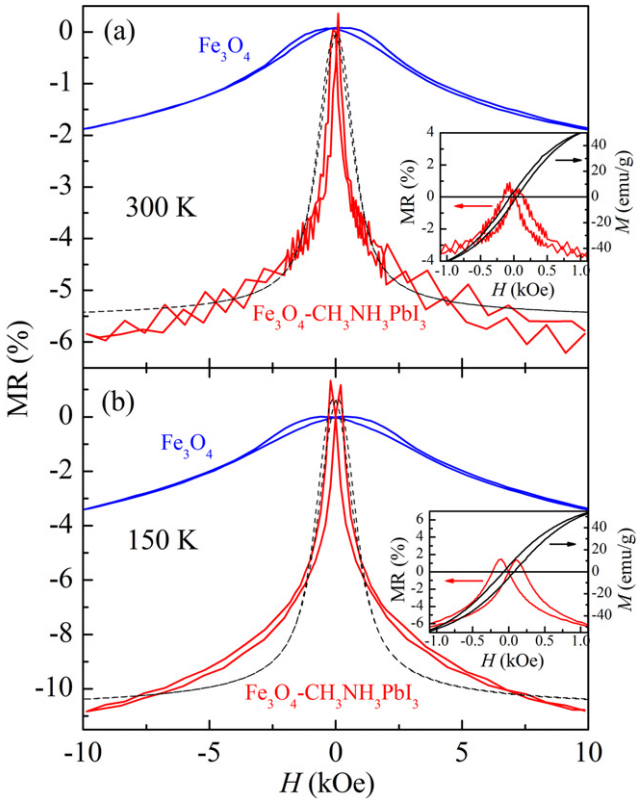

Figure 5. The field dependent MR for Fe_3O_4 particles with and without $CH_3NH_3PbI_3$ coating at (*a*) 300 K and (*b*) 150 K. The dashed line is the fitting with MR$\propto -(M/M_s)^2$. The insets show the low field MR curves and corresponding M–H curves for $CH_3NH_3PbI_3$-coated Fe_3O_4 particles.

Figure 5 shows the field dependent MR for Fe_3O_4 particles with and without $CH_3NH_3PbI_3$ coating measured at 300 K and 150 K. MR is defined as $[R(H) - R(0)] \times 100\%/R(0)$, where $R(0)$ and $R(H)$ are the resistivity in zero field and the applied field, respectively. As can be seen in figure 5(*a*), the MR value of pure Fe_3O_4 particles is only -1.9% under a field of 10 kOe, which increases to about -6% for the $CH_3NH_3PbI_3$-coated Fe_3O_4 particles at 300 K. Furthermore, the $CH_3NH_3PbI_3$-coated Fe_3O_4 particles show a much larger low field MR value, -3.8% under 1 kOe (only -0.1% for pure Fe_3O_4 particles). The MR increases with decreasing temperature. The MR for the pure Fe_3O_4 particles increases to -3.4%, while -10.8% for the $CH_3NH_3PbI_3$-coated Fe_3O_4 particles at 150 K, as shown in figure 5(*b*). The MR at 1 kOe is -5.6%, which is much larger than that of pure Fe_3O_4 particles (-0.27%). Generally organic materials have weak spin–orbit interaction, leading to very long spin relaxation time and coherence length [5]. Though the spin coherent length has not yet been determined for $CH_3NH_3PbI_3$, the electron–hole diffusion length has been measured to be about 100 nm [9]. Considering the estimated thickness of the $CH_3NH_3PbI_3$ coating ($\sim$30 nm), the spin coherent length might be much longer than 30 nm. Of course, further experiments are needed to determine the spin relaxation time and coherent length. Even though, the enhanced MR effect in our experiment clearly demonstrates that $CH_3NH_3PbI_3$ is an appropriate candidate organic material to be applied in spintronics.

In magnetic granular films, the MR can be understood by the magnetic field adjusted transmission coefficient between the neighbouring particles which depends on the relative orientation of each magnetization [6, 15]. The spin polarization P can be roughly estimated from the saturated MR value with the equation MR $= P^2/(1 + P^2)$ [15]. We can estimate the P for Fe_3O_4 is 25.3% at 300 K, and 34.8% at 150 K, which is much smaller than the expected spin polarization for Fe_3O_4 (experimentally 80% and theoretically up to 100%) [12]. This might be due to the unsaturated MR curve even at 10 kOe, although the magnetization has saturated already. Furthermore, the unsaturated MR curves don't follow the relation MR$\propto -(M/M_s)^2$. All these features suggest that the surface spin disorder is crucial to determine the MR especially for small particles, as suggested in previous literature that the MR effect is an interface effect [3]. $CH_3NH_3PbI_3$ between Fe_3O_4 particles can effectively separate Fe_3O_4 particles, leading to the easy orientation of the surface magnetization of Fe_3O_4 particles by the magnetic field, otherwise the interaction between the contacting Fe_3O_4 particles will hinder the change of the relative orientation of the surface magnetization. This can be seen that the field of the MR peak for $CH_3NH_3PbI_3$-coated Fe_3O_4 particles is much smaller than that for pure Fe_3O_4 [16]. It has been reported that the MR effect strongly depends on the interfacial spin states, which is due to the hybridization between the FM electrodes and the organic spacer [17]. A similar phenomenon has also been observed in other organic coated Fe_3O_4 systems, that the magnetization was easy to saturate while the MR was difficult to saturate [3]. Though the shape of the M–H curves of the Fe_3O_4 particles with and without $CH_3NH_3PbI_3$ coating is similar, the MR curve of $CH_3NH_3PbI_3$-coated Fe_3O_4 particles has a much larger slope at low fields, indicating the possible suppression of the spin disorder at the surface of the Fe_3O_4 particles [18], while the slopes at high fields are nearly the same. The deterioration of spin polarization might also be due to the polycrystalline nature of Fe_3O_4 particles. The application of a $CH_3NH_3PbI_3$ spacer can efficiently overcome the spin scattering at the particle boundaries, but the spin scattering at the grain boundaries inside the particles still exists, which might deteriorate the total spin polarization of Fe_3O_4. Thus single crystalline Fe_3O_4 particles will be further applied to improve the MR effect.

In summary, $CH_3NH_3PbI_3$ has been applied to coat the Fe_3O_4 particles. The MR is about -6% at 300 K and -10.8% at 150 K under magnetic field of 10 kOe, which is about 3 times larger than the value of pure Fe_3O_4 (-1.9% at 300 K and -3.4% at 150 K). Furthermore, the low field MR (value under a magnetic field of 1 kOe) is more strongly enhanced (-3.8% at 300 K and -5.6% at 150 K). Our results clearly demonstrate that $CH_3NH_3PbI_3$ is a potential spin transport matrix in organic spintronics, which might also be true for other organometal trihalide perovskites.

Acknowledgments

This work is supported by the State Key Programme for Basic Research of China (2010CB923404, 2011CB922101),

the National Natural Science Foundation of China (51172044, 51322206, 11274060), the Natural Science Foundation of Jiangsu Province of China (BK2011617), the 333 project of Jiangsu province, the Scientific Research Foundation for the Returned Overseas Chinese Scholars, State Education Ministry.

References

[1] Baibich M N, Broto J M, Fert A, Nguyen Van Dau F, Petroff F, Eitenne P, Creuzet G, Friederich A and Chazelas J 1988 Giant magnetoresistance of (0 0 1)Fe/(0 0 1)Cr magnetic superlattices *Phys. Rev. Lett.* **61** 2472–5

[2] Žutić I, Fabian J and Das Sarma S 2004 Spintronics: fundamentals and applications *Rev. Mod. Phys.* **76** 323–410

[3] Wang S, Yue F J, Wu D, Zhang F M, Zhong W and Du Y W 2009 Enhanced magnetoresistance in self-assembled monolayer of oleic acid molecules on Fe_3O_4 nanoparticles *Appl. Phys. Lett.* **94** 012507

[4] Xu W, Szulczewski G J, LeClair P, Navarrete I, Schad R, Miao G, Guo H and Gupta A 2007 Tunneling magnetoresistance observed in $La_{0.67}Sr_{0.33}MnO_3$/organic molecule/Co junctions *Appl. Phys. Lett.* **90** 072506

[5] Wang S, Shi Y J, Lin L, Chen B B, Yue F J, Du J, Ding H F, Zhang F M and Wu D 2011 Room-temperature spin valve effects in $La_{0.67}Sr_{0.33}MnO_3$/Alq_3/Co devices *Synth. Met.* **161** 1738–41

[6] Naber W J M, Faez S and van der Wiel W G 2007 Organic spintronics *J. Phys. D: Appl. Phys.* **40** R205–28

[7] Liu M, Johnston M B and Snaith H J 2013 Efficient planar heterojunction perovskite solar cells by vapour deposition *Nature* **501** 395–8

[8] Heo J H, Im S H, Noh J H, Mandal T N, Lim C, Chang J A, Lee Y H, Sarkar A, Nazeeruddin Md K, Grätzel M and Seok S I 2013 Efficient inorganic–organic hybrid heterojunction solar cells containing perovskite compound and polymeric hole conductors *Nature Photon.* **7** 486–91

[9] Stranks S D, Eperon G E, Grancini G, Menelaou C, Alcocer M J P, Leijtens T, Herz L M, Petrozza A and Snaith H J 2013 Electron–hole diffusion lengths exceeding 1 micrometer in an organometal trihalide perovskite absorber 2013 *Science* **342** 341–4

[10] Deng H, Li X, Peng Q, Wang X, Chen J and Li Y Monodisperse magnetic single-crystal ferrite microspheres 2005 *Angew. Chem. Int. Edn* **44** 2782–5

[11] Noh J H, Im S H, Heo J H, Mandal T N and Seok S I 2013 Chemical management for colorful, efficient, and stable inorganic–organic hybrid nanostructured solar cells *Nano Lett.* **13** 1764–9

[12] Liu W Q, Xu Y B, P. Wong K J, Maltby N J, Li S P, Wang X F, Du J, You B, Wu J, Bencok P and Zhang R 2014 Spin and orbital moments of nanoscale Fe_3O_4 epitaxial thin film on MgO/GaAs(1 0 0) 2014 *Appl. Phys. Lett.* **104** 142407

[13] Lu A, Salabas E L and Schüth F 2007 Magnetic nanoparticles: synthesis, protection, funtionalization, and application *Angew. Chem. Int. Edn* **46** 1222–44

[14] Sethulakshmi N, Sooraj V, Sajeev U S, Nair S S, Narayanan T N, Joy L K, Joy P A, Ajayan P M and Anantharaman M R 2013 Contact potential induced enhancement of magnetization in polyaniline coated nanomagnetic iron oxides by plasma polymerization *Appl. Phys. Lett.* **103** 162414

[15] Inoue J and Maekawa S 1996 Theory of tunneling magnetoresistance in granular magnetic films 1996 *Phys. Rev.* B **53** R11927–9

[16] Yue F J, Wang S, Lin L, Zhang F M, Li C H, Zuo J L, Du Y W and Wu D Large low-field magnetoresistance in Fe_3O_4/molecule nanoparticles at room temperature 2011 *J. Phys. D: Appl. Phys.* **44** 025001

[17] Jiang S W, Shu D J, Lin L, Shi Y J, Shi J, Ding H F, Du J, Wang Mu and Wu D 2014 Strong asymmetrical bias dependence of magnetoresistance in organic spin valves: the role of ferromagnetic/organic interfaces *New J. Phys.* **16** 013028

[18] Cótica L F, Santos I A, Girotto E M, Ferri E V and Coelho A A 2010 Surface spin disorder effects in magnetite and poly(thiophene)-coated magnetite nanoparticles *J. Appl. Phys.* **108** 064325